

# Template Assembled Synthetic Proteins (TASPs). Are Template Size, Shape, and Directionality Important in Formation of Four-Helix Bundles?

Allan K. Wong,<sup>†</sup> Michael P. Jacobsen,<sup>‡</sup> Donald J. Winzor,<sup>‡</sup> and David P. Fairlie<sup>\*,†</sup>

Contribution from the Centre for Drug Design and Development and Department of Biochemistry, The University of Queensland, Brisbane, Qld 4072, Australia

Received June 13, 1997

**Abstract:** A series of *rigid* aromatic templates that vary in size, shape, and directionality have been investigated in template-assembled synthetic 4 $\alpha$ -helix peptide bundles for their capacity to enhance the  $\alpha$ -helicity of an amphiphilic peptide (DAATALANALKKL-[NHCH<sub>2</sub>CH<sub>2</sub>SH]). In aqueous phosphate buffer (10 mM, pH 7) the peptide has some innate helicity (~30%) which is concentration-independent between 1 and 250  $\mu$ M. Helicity is enhanced to 64–75% when 4 equiv of the peptide are connected to aromatic templates based on benzene, benzanilide, or a cyclic octapeptide. This effect is concentration-independent by circular dichroism spectroscopy (3–60  $\mu$ M [TASP]), the TASPs are monomeric by sedimentation equilibrium experiments, and have comparable thermodynamic stabilities. Thus these templates induce *intra*- rather than *inter*- molecular peptide association and are equally effective despite variations in size, shape, and directionality. When the linker between the template and peptides is sufficiently long, as in these cases, TASP formation is less sensitive to the dimensions of the template than to the communication between hydrophobic peptide side chains, which are the main determinants of helix separation, 4 $\alpha$ -helix bundle size and stability. This greatly simplifies approaches to developing small molecule mimetics of *interacting* protein surfaces. However template size, shape, and directionality may still be important when the linker is short or when assembled peptide surfaces are isolated from one another and unable to communicate.

## Introduction

One of the great challenges in chemistry is to reproduce the bioactivities of proteins using smaller molecular structures.<sup>1</sup> Toward the goal of structurally mimicking discontinuous bioactive peptide surfaces brought together through folding, early research has focused on Template-Assembled Synthetic Proteins (TASP)<sup>2,1d</sup> in which short amphiphilic peptides are assembled into three or four  $\alpha$ -helix bundles on templates such

as flexible linear<sup>2b,c,i,3</sup> and cyclic<sup>2d,e,h,4</sup> peptides, and more rigid porphyrins,<sup>5</sup> cavitands,<sup>6</sup> and metal ions.<sup>7</sup> These templates have been found to enhance the peptide helicity, an effect attributed to *intramolecular* peptide association within a single TASP.

The formation of intramolecular four-helix bundles is often inferred from the concentration-independence of circular dichroism spectra. Yet this observation could also result from *intermolecular* peptide association between two or more strongly interacting TASPs in the  $\mu$ M concentration ranges studied, if the dissociation constant <  $\mu$ M. Moreover, templates used to date have been synthetically too complex to easily vary template dimensions. Consequently the influence of template size, shape, and directionality on TASP formation remains to be fully

<sup>†</sup> Centre for Drug Design and Development.

<sup>‡</sup> Department of Biochemistry.

(1) (a) Ho, S. P.; DeGrado, W. F. *J. Am. Chem. Soc.* **1987**, *109*, 6751–6758. (b) Regan, L.; DeGrado, W. F. *Science* **1988**, *241*, 976–978. (c) Schneider, J. P.; Kelly, J. W. *Chem. Rev.* **1995**, *95*, 2169–2187. (d) Fairlie, D. P.; West, M. L.; Wong, A. K. *Curr. Med. Chem.* **1998**, *5*, 29–62.

(2) (a) Mutter, M.; Vuilleumier, S. *Angew. Chem., Int. Ed. Engl.* **1989**, *28*, 535–676. (b) Mutter, M.; Altmann, K.-H.; Tuchscherer, G.; Vuilleumier, S. *Tetrahedron* **1988**, *44*, 771–785. (c) Mutter, M.; Hersperger, R.; Gubernator, K.; Muller, K. *Proteins* **1989**, *5*, 13–21. (d) Ernest, I.; Vuilleumier, S.; Fritz, H.; Mutter, M. *Tetrahedron Lett.* **1990**, *28*, 4015–4018. (e) Mutter, M.; Tuchscherer, G.; Miller, C.; Altmann, K.-H.; Carey, R. I.; Wyss, D. F.; Labhardt, A. M.; Rivier, J. E. *J. Am. Chem. Soc.* **1992**, *114*, 1463–1470. (f) Tuchscherer, G.; Dörner, B.; Sila, U.; Kamber, B.; Mutter, M. *Tetrahedron* **1993**, *49*, 3559–3575. (g) Ernest, I.; Kalvoda, J.; Sigel, C.; Rihs, G.; Fritz, H.; Blommers, M. J. J.; Raschdorf, F.; Francotte, E.; Mutter, M. *Helv. Chim. Acta* **1993**, *76*, 1539–1563. (h) Grove, A.; Mutter, M.; Rivier, J. E.; Montal, M. *J. Am. Chem. Soc.* **1993**, *115*, 5919–5924. (i) Nyanguile, O.; Mutter, M.; Tuchscherer, G. *Lett. Peptide Science* **1994**, *1*, 9–16. (j) Dumy, P.; Eggleston, I. M.; Cervigni, S.; Sila, U.; Sun, X.; Mutter, M. *Tetrahedron Lett.* **1995**, *36*, 1255–1258. (k) Tuchscherer, G.; Mutter, M. *J. Peptide Science* **1995**, *1*, 3–10. (l) Nefzi, A.; Sun, X.; Mutter, M. *Tetrahedron Lett.* **1995**, *36*, 229–230.

(3) Dawson, P. E.; Kent, B. H. *J. Am. Chem. Soc.* **1993**, *115*, 7263–7266.

(4) (a) Arai, T.; Ide, Y.; Tanaka, Y.; Fujimoto, T.; Nishino, N. *Chem. Lett.* **1995**, 381–82. (b) Matsubara, A.; Asami, K.; Akagi, A.; Nishino, N. *J. Chem. Soc. Chem. Commun.* **1996**, 2069–70. See also ref 1d.

(5) *Four-helix Bundles*: (a) Sasaki, T.; Kaiser, E. T. *J. Am. Chem. Soc.* **1989**, *111*, 380–381. (b) Sasaki, T.; Kaiser, E. T. *Biopolymers* **1990**, *295*, 79–88. (c) Ghadiri, M. R.; Soares, C.; Choi, C. *J. Am. Chem. Soc.* **1992**, *114*, 4000–4002. (d) Akerfeldt, K. S.; Kim, R. M.; Camac, D.; Groves, J. T.; Lear, J. D.; DeGrado, W. F. *J. Am. Chem. Soc.* **1992**, *114*, 9656–9657. (e) Choma, C.; Lear, J.; Nelson, M.; Dutton, P.; Robertson, D.; DeGrado, W. *J. Am. Chem. Soc.* **1994**, *116*, 856–865. (f) Gibb, B. C.; Mezo, A. R.; Causton, A. S.; Fraser, J. R.; Tsai, F. C. S.; Sherman, J. C. *Tetrahedron* **1995**, *51*, 8719–8732. See also ref 1d.

(6) Gibb, B. C.; Mezo, A. R.; Causton, A. S.; Fraser, J. R.; Tsai, F. C. S.; Sherman, J. C. *Tetrahedron* **1995**, *51*, 8719–8732.

(7) *3-Helix Bundles*: (a) Lieberman, M.; Sasaki, T. *J. Am. Chem. Soc.* **1991**, *113*, 1470–1471. (b) Ghadiri, M. R.; Case, M. A. *Angew. Chem., Int. Ed. Engl.* **1993**, *32*, 1594–1597. (b) Ghadiri, M. R.; Soares, C.; Choi, C. *J. Am. Chem. Soc.* **1992**, *114*, 4000–4002. (d) Sasaki, T.; Lieberman, M. *Tetrahedron* **1993**, *49*, 3677–3689. (e) Lieberman, M.; Tabet, M.; Sasaki, T. *J. Am. Chem. Soc.* **1994**, *116*, 5035–5044.

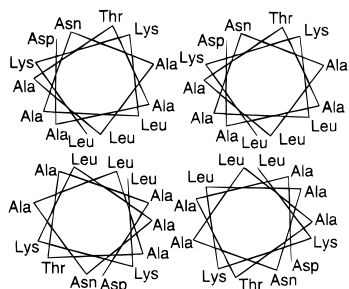
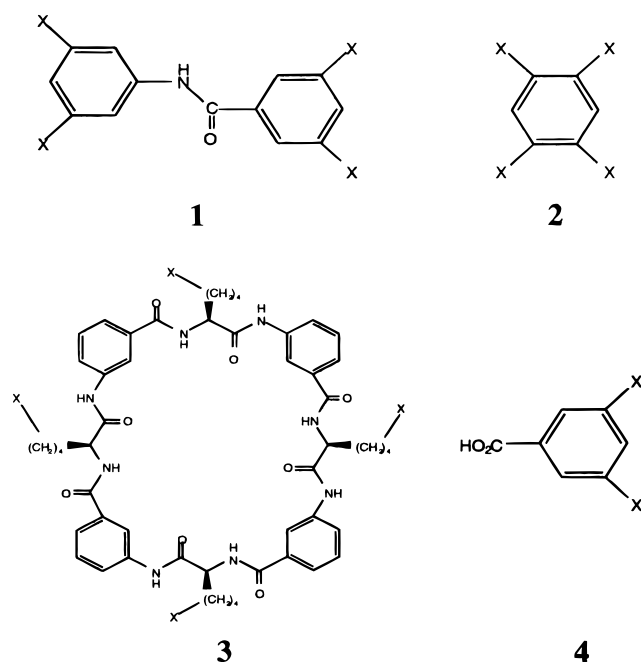


**Figure 1.** Helical wheels for 4 equivs of peptide **5**.

elucidated. We have begun to investigate these effects and the molecular nature of TASPs using a series of simple templates composed of rigid units (**1–4**, X = NHCOCH<sub>2</sub>Br) attached to up to 4 equiv of a cysteamine-linked peptide (**5**, DAATA-LANALKKL-[NHCH<sub>2</sub>CH<sub>2</sub>SH]) which is known to have some helical propensity.<sup>3</sup>



Templates **1–4** were chosen for this study because of their simplicity, ease of varying size and shape, and because of the known sizes of 4 $\alpha$ -helix bundles in proteins. Proteins with 4 $\alpha$ -helix bundles have very different interhelix distances between axes (6–16 Å but commonly 10  $\pm$  3 Å)<sup>8</sup> depending upon the packing requirements for their different sized hydrophobic peptide side chains. Packing of four helices into a bundle requires four pairs of interacting surfaces as shown in the helical wheel for peptide **5** (Figure 1). From estimated minimum Leu...Leu (~13 Å), Ala...Ala (~8 Å), or Leu...Ala (~11 Å) separations, we expected that this bundle would either be rectangular (13  $\times$  8 Å) or square (11  $\times$  11 Å), compared with the approximate dimensions of templates **1–3** of 12  $\times$  9, 6.5  $\times$  9, and 9  $\times$  9 Å, respectively. Unlike templates **1** and **2**, template **3** has the additional perceived advantage of orienting all four peptide chains in the same direction. So if there is an advantage of designing templates with complementary size, shape, or directionality for the four-helix bundle, this should be reflected in different stabilities for TASPs composed of these templates.

(8) Reddy, B. V. B.; Blundell, T. L. *J. Mol. Biol.* **1993**, *233*, 464–479.

## Results and Discussion

The peptide **5** chosen for this study of template-assembled synthetic proteins is similar to that previously condensed onto a flexible peptide template,<sup>3</sup> except that the C-terminal glycine is replaced by cysteamine. This modification<sup>9</sup> was effected by reacting 4-hydroxymethylphenoxy acetic acid with cysteamine·HCl in neat TFA to give the thioether-linked phenoxy acetic acid and after N-protecting (Scheme 1), this is coupled onto an aminomethylated polystyrene resin using HBTU/DIEA activation. Any remaining free sites are acetylated with acetic anhydride/DIEA before assembling the peptide **5** on the linker-resin.

The simple templates **1**, **2**, and **4** (X = NHCOCH<sub>2</sub>Br) were constructed from their amine precursors (X = NH<sub>2</sub>)<sup>10</sup> by reaction with excess bromoacetyl bromide in the presence of base. Template **3** was prepared by solution phase coupling of two dipeptide units to give the tetrapeptide, then coupling of 2 equiv of tetrapeptide to give the linear octapeptide, followed by cyclization with BOP, deprotection with HF, and bromoacetylation with bromoacetic acid and DCC (see Experimental Section).

Each of the resulting templates **1–4** (X = NHCOCH<sub>2</sub>Br) was then reacted in DMF/Tris buffer (pH 8.5) under argon with up to 4 equiv of the thiol-bearing peptide **5**, the thiolate nucleophile displacing bromide to form the corresponding TASPs **6–9** (X = NHCOCH<sub>2</sub>-**5**) which were characterized using rp-HPLC and electrospray mass spectrometry (Figure 2). TASP formation was monitored by rp-HPLC (20–50% gradient, 50 min, 0.1% TFA:90% CH<sub>3</sub>CN/H<sub>2</sub>O) and electrospray mass spectrometry for 100  $\mu$ L aliquots (quenched with 50  $\mu$ L of 0.5% TFA/H<sub>2</sub>O) removed at intervals from the reaction mixture. For example Figure 3 shows the formation of TASP **6** and various intermediates from template **1**. There is (i) no free template after 20 min of reaction, (ii) a complex mixture at all stages of the reaction (making isolation of intermediates difficult under these conditions), and (iii) a quantitative yield of TASP **6** within 130 min.

Figure 4 compares CD spectra for TASPs **6–9** and peptide **5** at equivalent peptide concentrations (24  $\mu$ M). TASPs **6–8** give prominent double minima (222, 208 nm) and a maximum (190 nm) characteristic of  $\alpha$ -helicity, while TASP **9** and peptide **5** have a dominant minimum at ~208 nm indicative of random coil. Using the mean residue ellipticity (MRE) at 222 nm, the peptide helicity was calculated<sup>11</sup> for the TASPs as 75% (**6**), 64% (**7**), 65% (**8**), 39% (**9**) versus 32% (**5**). Thus at this concentration, templates **1–3** promote  $\alpha$ -helix formation, whereas **4** does not. The MRE ratio (222/208 nm) may be indicative of the compactness of helices, ~1.0 being compact and ~0.75 for a loose helix.<sup>12</sup> The ratios (0.96 (**6**), 0.98 (**7**), 0.89 (**8**), 0.75 (**9**), 0.73 (**5**)) are consistent with high helicity for TASPs **6–8** only.

The helicities of TASPs **6–9** (3–60  $\mu$ M) and peptide **5** (1–250  $\mu$ M) were not concentration dependent, so the compounds are all thermodynamically stable under the experimental condi-

(9) Engelbretsen, D. R.; Garnham, B. G.; Bergman, D. A.; Alewood, P. F. *Tetrahedron Lett.* **1995**, *36*, 8871–8874.

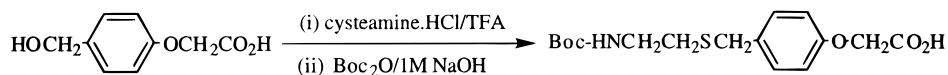
(10) Himeshima, Y.; Uemura, T.; Kurihara, M. *Jpn. Kokai Tokkyo Koho JP 62, 169, 754 [87, 169, 754] 25 July 1987*, Patent Appl. 86/10, 582, 21 Jan 1986.

(11) Chen, Y.-H.; Yang, J. T.; Chau, K. H. *Biochemistry* **1974**, *13*, 3350–3359.

(12) (a) Zhou, N. E.; Kay, C. M.; Hodges, R. S. *Biochemistry* **1992**, *31*, 5739–5746. (b) Garcia-Echeverria, C. *J. Am. Chem. Soc.* **1994**, *116*, 6031–6032.

(13) Wills, P. R.; Jacobsen, M. P.; Winzor, D. J. *Biopolymers* **1996**, *38*, 119–130.

## Scheme 1



tions. The concentration independence is consistent with, but not proof of, intramolecular association of the peptides in TASP 6–8, since the possibility remains that these TASP 6–8 are already highly intermolecularly associated above 3  $\mu\text{M}$  concentrations. On the other hand, the TASP 9 formed from half template 4 shows no evidence of helical induction even though intermolecular association is theoretically possible for it too.

To establish definitively the intramolecular nature of TASP 6–8, we conducted sedimentation equilibrium experiments on 6  $\mu\text{M}$  TASP solutions to determine the molecular weights of

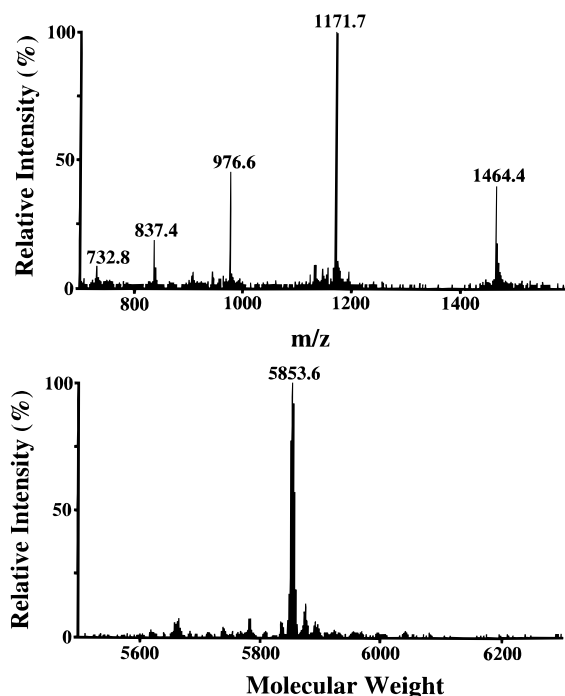


**Figure 2.** (top) Electrospray mass spectrum for TASP 6 formed from template 1 and peptide 5 showing  $m/z$  for multiple charge states ( $z = 4+$  to  $8+$ ); (bottom) reconstructed molecular weight from  $m/z$  peaks.

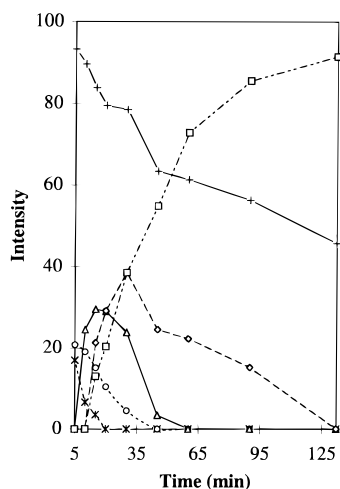


**Figure 3.** Time-dependent reaction of 0.3 mg (0.54  $\mu\text{mol}$ ) template 1 ( $\times$ ) with 3.66 mg (2.7  $\mu\text{mol}$ ) peptide 5 (+) in Tris buffer (1.35 mL, pH 8.5) and dioxane (1.35 mL) under Ar at 20  $^{\circ}\text{C}$ . Product distribution is shown for complexes of template plus one (o), two ( $\Delta$ ), three ( $\diamond$ ), or four ( $\square$ ) equivalents of peptide.

TASP 6–8 under the conditions used for the circular dichroism studies. Sedimentation equilibrium distributions for the TASP 6–8 are presented in Figure 5. Linear regression analyses of the dependence of  $A_{230}(r)$  upon  $\exp(r^2 - r_m^2)$  yielded values ( $\pm 2$  S.D.) of 0.76 ( $\pm 0.04$ ) for TASP 6 (Figure 5a), 0.68 ( $\pm 0.03$ ) for TASP 7 (Figure 5b), and 0.73 ( $\pm 0.04$ ) for TASP 8 (Figure 5c) for the reduced molecular weight ( $\phi M$  in eq 1 of Experimental Section) and hence molecular weights of 5900 ( $\pm 300$ ), 5300 ( $\pm 200$ ) and 5600 ( $\pm 300$ ) for TASP 6–8, respectively. Given the uncertainty in the estimate of solute partial specific volume, which only takes account of the polypeptide contribution, these approximate molecular weights compare favorably with the real values of 5851 (TASP 6), 5732 (TASP 7), and 6551 (TASP 8) deduced from chemical composition.

Sedimentation equilibrium experiments have thus established that the three TASP 6–8 are essentially monomeric under the experimental conditions used for the circular dichroism studies. Inspection of the residual plot in Figure 5c shows the adequacy of the description of TASP 8 as a monomer. Furthermore, although some association of TASP 6 and TASP 7 is evident from the disparity between experimental and theoretical distributions in the vicinity of the cell base (Figure 5 (parts a and b) respectively), the sedimentation behavior is symptomatic of a very small extent of irreversible aggregation.

Two approaches have been used to eliminate the possibility of the discrepancy being a consequence of reversible self-association: (i) direct analysis of the sedimentation equilibrium distributions by means of the psi function<sup>13</sup> indicated a value of unity for the proportion of monomeric material at radial positions of 6.95, 7.00, 7.05, and 7.10 cm but a value of 0.7–0.8 for the proportion at the bottom of the liquid column. The absence of a systematic decrease in this proportion with radial distance, which would be commensurate with reversible self-association, can be ascertained from the high conformity between the experimental and theoretical distributions for almost the entire column length (Figure 5 (parts a and b)); (ii) additional evidence for stability of the monomeric state of TASP 7, the sample exhibiting greatest heterogeneity in Figure 5, is provided by analysis of the sedimentation equilibrium distribution (Figure 6) from an experiment using a 10-fold higher TASP concentration (60  $\mu\text{M}$  vs 6  $\mu\text{M}$ ). An apparent molecular weight of 5300

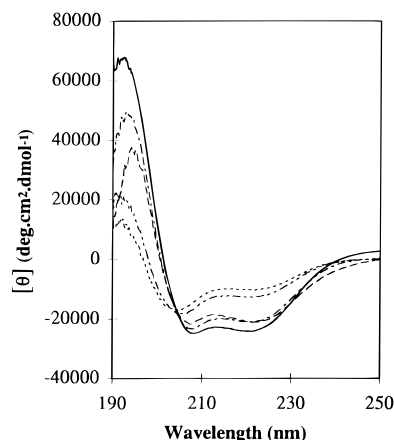


**Figure 4.** Circular dichroism spectra. Mean residue ellipticity ( $\theta$ ) decreases at 210 nm in the order 5 > TASP 7 > 8 > 6 in 10 mM phosphate buffer (pH 7) at 20  $^{\circ}\text{C}$ .

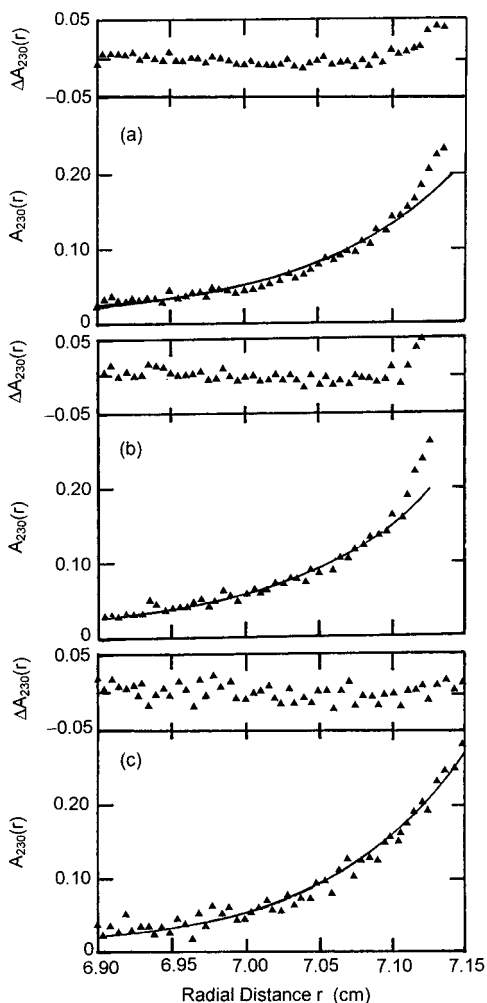


**Figure 5.** Sedimentation equilibrium experimental distributions ( $\blacktriangle$ ) at 50 000 rpm and 20 °C for 6  $\mu$ M solutions of (a) TASP 6, (b) TASP 7, and (c) TASP 8 in 10 mM phosphate buffer, pH 7. Solid lines are the best fit descriptions in terms of a single solute. The degree of goodness of fit to such descriptions is shown by the residual plot (upper panel) in each case.

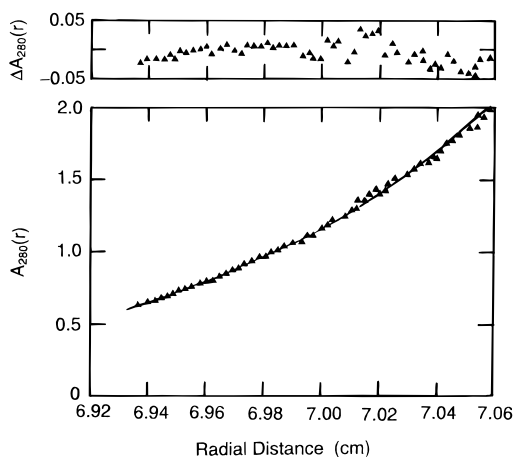


**Figure 6.** Sedimentation equilibrium experimental distributions ( $\blacktriangle$ ) at 50 000 rpm and 20 °C for 60  $\mu$ M TASP 7 in 10 mM phosphate buffer (pH 7). The solid line is the best fit description in terms of a single solute with MW = 5300, and the upper panel presents the residual plot to signify the goodness of fit.

( $\pm 200$ ) is inferred from the radial dependence of absorbance readings below 1.5 in terms of eq 1 (see Experimental Section). Because the solute concentration in the vicinity of the meniscus

**Table 1.** Denaturation of TASPs in Guanidine·HCl

protein	$C_{0.5}^a$ (M)	$\Delta G_{H_2O}^b$ (kcal mol $^{-1}$ )	$-m^c$ (kcal mol $^{-1}$ M $^{-1}$ )
<b>6</b>	1.4	-3.6	2.7
<b>7</b>	1.4	-3.4	2.3
<b>8</b>	1.4	-4.2	3.2
helichrome $^d$	5.2	-4.4	0.8

$^a$  [GnHCl] to denature 50% TASP at 22 °C.  $^b$  Free energy change for unfolding in absence of denaturant.  $^c$  Slope of  $\Delta G_{obs}$  versus [GnHCl], where  $\Delta G_{obs}$  ( $= -RT \ln K_{obs}$ ) is the free energy of unfolding at different concentrations of GnHCl.  $^d$  Synthetic 4 $\alpha$  protein, see ref 5b.

in Figure 6 already exceeds that at the cell base of the experiment shown in Figure 5b, the high molecular weight material detected in the earlier distribution cannot reflect reversible self-association.

To further understand whether there is an advantage in designing templates that are complementary to the four-helix bundle, we examined the relative thermodynamic stabilities of the TASPs 6–8. CD spectroscopy was used to monitor the decrease in peptide  $\alpha$ -helicity of 6–8 in the presence of increasing concentrations of guanidine·HCl. From the resulting denaturation profiles we determined the concentration of guanidine·HCl required to denature 50% of each TASP ( $C_{0.5}$ , Table 1). This is independent of the template and lower than required to denature other more amphiphilic proteins that also contain more polar amino acids. $^{5b}$  We also calculated the free energies of stabilization ( $\Delta G_{H_2O}$ , Table 1) for each TASP in the absence of denaturant as described in the Experimental Section. These thermodynamic stabilities ( $\Delta G_{H_2O}$ ) are similar in magnitude for 6–8 and similar to those reported for both native proteins $^{5b}$  such as  $\alpha$ -lactalbumin (-4.2), ribonuclease (-7.5), myoglobin (-7.6), and lysozyme (-8.9 kcal/mol), as well as some designed proteins. $^{5b,c,7b}$  Therefore we conclude that the flexible linker between the template and peptide(s) is sufficiently long in our examples to overcome any limitations placed by the size and shape of the template on interhelical peptide communication. Indeed the magnitude of the slope of these denaturation plots ( $m$ , Table 1), thought to be an indicator of the extent of cooperativity between peptides, $^{14}$  is similar for other native and synthetic proteins $^{5b}$  and suggests a high degree of interhelical peptide interaction in TASPs 6–8.

In summary these results establish that, for suitably long linkers, the *shape*, *size*, and *directionality* of the template are not critical for 4 $\alpha$ -helix TASP formation. Template 3, which can direct the attached peptides perpendicular to the “plane” of the cyclic peptide, was no more effective than the “directionless” templates 1 or 2 in inducing helicity. This is consistent with interhelical peptide associations being the main driving force for four-helix bundle formation. Following this work we became aware of the use of template 3 in another four-helix TASP $^4$  with a peptide $^{4a}$  having even larger packing requirements (13  $\times$  13 Å) than here due to four pairs of Leu $\cdots$ Leu surfaces. Thus the dimensions of the template do not need to precisely match those of the four-helix bundle but should not be so different as to prevent its formation through intramolecular peptide interactions. This greatly simplifies approaches to developing small molecule mimetics of *interacting* protein surfaces, such as helix bundles and associating loops. However template size, shape, and directionality are expected to become important in determining the thermodynamic stability of the TASP when the linker is short or when assembled peptide surfaces are isolated from one another and/or not communicating.

(14) Green, R. F., Jr.; Pace, C. N. *J. Biol. Chem.* **1974**, *249*, 5388–5393.

## Experimental Section

**Abbreviations.** DIEA = diisopropylethylamine; DMF = *N,N*-dimethylformamide; BOP = [Benzotriazol-1-yloxytris(dimethylamino)-phosphonium]hexafluorophosphate; TFA = trifluoroacetic acid; HBTU = (2-(1H-benzotriazol-1-yl)-1,1,3,3-tetramethyluronium)hexafluorophosphate; DCC = 1,3-dicyclohexylcarbodiimide; Tris = tris(hydroxymethyl)aminomethane; CIZ = 2-chlorobenzoyloxycarbonyl; mABA = metaaminobenzoic acid; GnHCl = guanidine hydrochloride.

**Materials and Methods.** Amino acids and aminomethylated polystyrene resin were purchased from Novabiochem. Other materials were obtained commercially as reagent grade. Gradient HPLC was carried out on Waters C-18 analytical (15  $\mu$ m, 8 mm  $\times$  100 mm) and semipreparative (15  $\mu$ m, 25 mm  $\times$  100 mm) columns. Analytical runs were 100% A for 2 min, then 0–60% B gradient over 60 min at 2 mL/min, where buffer A is 0.1% TFA in H<sub>2</sub>O and buffer B is 0.1% TFA in 90% CH<sub>3</sub>CN/H<sub>2</sub>O. <sup>1</sup>H and <sup>13</sup>C NMR spectra were recorded on a Varian Gemini 300 MHz NMR spectrometer and chemical shifts are reported in ppm relative to TMS in DMSO-*d*<sub>6</sub> or CDCl<sub>3</sub>. Reverse phase HPLC was carried out on Waters Delta-Pak PrepPak C<sub>18</sub> analytical (15  $\mu$ m, 8 mm  $\times$  100 mm) and semipreparative (15  $\mu$ m, 25 mm  $\times$  100 mm) columns using gradient mixtures of water/0.1% TFA/acetonitrile. Analytical runs were 0–50% B gradient over 30 min at 2 mL/min where buffer A is 0.1% TFA in H<sub>2</sub>O and buffer B is 0.1% TFA in 90% CH<sub>3</sub>CN/H<sub>2</sub>O.

Mass spectra were obtained on a triple quadrupole mass spectrometer (PE SCIEX API III) equipped with an Ionspray (pneumatically assisted electrospray)<sup>15</sup> atmospheric pressure ionization source (ISMS). Solutions of compounds in 9:1 acetonitrile/0.1% aqueous trifluoroacetic acid were injected by syringe infusion pump at  $\mu$ M-pM concentrations and flow rates of 2–5  $\mu$ L/minute into the spectrometer. Molecular ions,  $\{[M + nH]^{n+}\}/n$ , were generated by the ion evaporation process<sup>16</sup> and focused into the analyzer of the mass spectrometer through a 100 mm sampling orifice. Full scan data was acquired by scanning quadrupole-1 from *m/z* 100–900 with a scan step of 0.1 dalton and a dwell time of 2 ms. Accurate mass determinations were performed on a KRATOS MS25 mass spectrometer using Electron Impact ionization.

**Template Synthesis. 3,5-Di(bromoacetamido)-*N*-(3,5-di(bromoacetamido)phenyl)benzamide (1).** 3,5-Diamino-*N*-(3,5-diaminophenyl)benzamide<sup>10</sup> (64 mg, 0.249 mmol) was dissolved in dry THF (2 mL). This solution was then added to a mixture of bromoacetyl bromide (0.095 mL, 1.1 mmol), dry THF (2 mL), and triethylamine (0.168 mL, 1.2 mmol) and stirred for 2 h. The solvent was removed in vacuo, and the residue taken up into ethyl acetate (10 mL) and extracted with 3 M HCl (2  $\times$  10 mL), saturated NaHCO<sub>3</sub> (2  $\times$  10 mL), and brine (1  $\times$  5 mL), dried (MgSO<sub>4</sub>), and filtered, and the solvent was removed in vacuo to give an off-white powder (0.110 g, 60%). MS: 741.8 (M + H). <sup>1</sup>H NMR (DMSO-*d*<sub>6</sub>)  $\delta$  4.03 (s, 4H), 4.05 (s, 4H), 7.74 (t, *J* = 2.0 Hz, 1H), 7.77 (d, *J* = 1.7 Hz, 2H), 7.82 (d, *J* = 1.7 Hz, 2H), 8.17 (t, *J* = 2.0 Hz, 1H), 10.48 (s, 3H), 10.64 (s, 2H). <sup>13</sup>C NMR (DMSO-*d*<sub>6</sub>)  $\delta$  31.9, 107.2, 108.3, 114.1, 115.5, 138.0, 140.3, 141.1, 166.2, 166.4, 171.4.

**1,2,4,5-Tetra(bromoacetamido)benzene (2).** 1,2,4,5-Benzenetetramine tetrahydrochloride (0.10 g, 0.35 mmol) was dissolved in *N,N*-dimethylacetamide (2.4 mL) and triethylamine (0.687 mL, 4.9 mmol). Bromoacetyl bromide (0.305 mL, 3.5 mmol) was added, and the mixture was stirred for 2 h. The mixture was concentrated in vacuo, taken up into ethyl acetate (20 mL), and extracted with 3 M HCl (2  $\times$  15 mL), saturated NaHCO<sub>3</sub> (2  $\times$  15 mL), and brine (1  $\times$  10 mL), dried (MgSO<sub>4</sub>), filtered, and dried. The product (2) was an off-white powder (0.165 g, 75%). MS: 621.8 (M + H)<sup>+</sup>. <sup>1</sup>H NMR (DMSO-*d*<sub>6</sub>)  $\delta$  4.10 (s, 4H), 4.31 (s, 4H), 7.75 (s, 2H), 9.67 (s, 1H), 9.72 (s, 1H), 9.76 (s, 1H), 9.82 (s, 1H). <sup>13</sup>C NMR (DMSO-*d*<sub>6</sub>)  $\delta$  31.4, 31.5, 122.3, 128.9, 166.6, 166.7.

**Boc-Lys(CIZ)-mABA-OMe (3a).** Boc-lysine(CIZ)-OH (2.52 g, 6.63 mmol) in DMF (15 mL) was stirred with HBTU (2.51 g, 6.63 mmol), DIEA (1.15 mL, 6.63 mmol), and *m*-aminobenzoic acid methyl ester (1.0 g, 6.63 mmol) for 15 h. The solvent was removed in vacuo, and the residue was taken up in ethyl acetate (90 mL), washed with 2 N

HCl (2  $\times$  25 mL), saturated NaHCO<sub>3</sub> (2  $\times$  25 mL) and brine (2  $\times$  20 mL), dried (Na<sub>2</sub>SO<sub>4</sub>), filtered, and concentrated in vacuo to give a brown gum **3a** (3.31 g, 91%). MS: 548.0 (M + H)<sup>+</sup>. <sup>1</sup>H NMR (CDCl<sub>3</sub>)  $\delta$  1.44 (s, 9H), 1.53 (m, 2H), 1.71 (m, 2H), 1.92 (m, 2H), 3.19 (m, 2H), 3.87 (s, 3H), 4.26 (s, 1H), 5.04 (s, 1H), 5.20 (s, 1H), 5.39 (s, 1H), 7.25 (m, 2H), 7.36 (m, 3H), 7.73 (d, *J* = 7.7 Hz, 1H), 7.79 (d, *J* = 7.7 Hz), 8.11 (s, 1H), 8.84 (s, 1H). <sup>13</sup>C NMR (CDCl<sub>3</sub>)  $\delta$  24.1, 29.9, 31.0, 32.8, 56.6, 65.7, 82.3, 122.3, 125.8, 126.9, 128.5, 130.6, 131.0, 131.1, 131.3, 132.4, 135.1, 135.7, 139.6, 157.9, 158.1, 168.3, 172.3.

**Boc-(Lys(CIZ)-mABA)<sub>2</sub>OMe (3b).** Boc-Lys(CIZ)-mABA-OH (2.10 g, 3.93 mmol), prepared by treatment of Boc-Lys(CIZ)-mABA-OMe (**3a**) with aqueous NaOH, was dissolved in DMF (10 mL). HBTU (1.49 g, 3.93 mmol) and DIEA (0.684 mL, 3.93 mmol) were added to the stirred solution, and then NH<sub>2</sub>-Lys(CIZ)-mABA-OMe (1.62 g, 3.61 mmol), which was prepared by treatment of **3a** with TFA/DCM, was added to the activated peptide. The mixture was stirred for 5 h, and the reaction was monitored by TLC (1:4 MeOH:CHCl<sub>3</sub>). The solution was concentrated in vacuo, dissolved in ethyl acetate (90 mL), washed with 1 N HCl (2  $\times$  20 mL), saturated NaHCO<sub>3</sub> (2  $\times$  20 mL), and brine (20 mL), dried (Na<sub>2</sub>SO<sub>4</sub>), and filtered, and solvent was removed in vacuo to give the tetrapeptide (**3b**, 3.4 g, 99%). MS: 963.1 (M + H)<sup>+</sup>. <sup>1</sup>H NMR (CDCl<sub>3</sub>)  $\delta$  1.44 (s, 9H), 1.54 (m, 8H), 1.90 (m, 4H), 3.18 (m, 4H), 3.85 (s, 3H), 4.39 (m, 1H), 4.91 (m, 1H), 5.13 (s, 4H), 7.27 (m, 12H), 7.62 (m, 1H), 7.70 (d, *J* = 7.5 Hz, 1H), 7.82 (m, 1H), 7.98 (m, 1H), 8.15 (s, 1H), 9.37 (s, 1H), 9.80 (s, 1H). <sup>13</sup>C NMR (CDCl<sub>3</sub>)  $\delta$  24.5, 29.8, 31.0, 33.7, 54.0, 56.6, 65.5, 82.1, 119.8, 122.5, 128.4, 130.6, 130.8, 130.9, 131.0, 131.1, 131.3, 132.0, 134.9, 135.8, 139.5, 139.9, 157.9, 158.0, 158.2, 168.9, 169.6, 172.4, 174.0.

**Boc-(Lys(CIZ)-mABA)<sub>4</sub>OMe (3c).** Boc-(Lys(CIZ)-mABA)<sub>2</sub>-OH (1.84 g, 1.94 mmol), prepared by treatment of **3b** with aqueous NaOH, was dissolved in DMF (10 mL). HBTU (0.735 g, 1.94 mmol) and DIEA (0.358 mL, 2.06 mmol) were added to the stirred solution, and then NH<sub>2</sub>-Lys(CIZ)-mABA<sub>2</sub>-OMe (1.68 g, 1.94 mmol), prepared by treating **3b** with TFA/DCM, was added to the activated peptide. The mixture was stirred for 5 h, and the reaction was monitored by TLC (1:4 MeOH:CHCl<sub>3</sub>). The solution was concentrated in vacuo, dissolved in ethyl acetate (90 mL), washed with 1 N HCl (2  $\times$  20 mL), saturated NaHCO<sub>3</sub> (2  $\times$  20 mL), and brine (20 mL), dried (Na<sub>2</sub>SO<sub>4</sub>), and filtered, and solvent was removed in vacuo to give the octapeptide as gum (3.15 g). This was recrystallized from CHCl<sub>3</sub>–toluene to give **3c** (3.08 g, 88%). MS: 1794.3 (M + H)<sup>+</sup>. <sup>1</sup>H NMR (MeOH-*d*<sub>4</sub>)  $\delta$  1.39 (m, 25H), 1.90 (m, 8H), 3.00 (m, 8H), 3.83 (s, 3H), 4.54 (m, 4H), 4.95 (s, 8H), 7.26 (m, 20H), 7.65 (m, 4H), 7.70 (m, 4H), 7.82 (m, 4H), 7.98 (m, 1H), 8.15 (s, 3H), 10.10 (s, 1H), 10.27 (s, 2H), 10.34 (s, 1H). <sup>13</sup>C NMR (MeOH-*d*<sub>4</sub>)  $\delta$  23.6, 29.3, 30.5, 33.3, 55.5, 56.0, 64.5, 80.6, 119.6, 121.9, 123.7, 124.9, 125.9, 127.7, 129.0, 129.8, 130.2, 130.5, 130.6, 130.7, 132.4, 134.0, 135.6, 135.7, 139.8, 157.3, 168.2, 168.9, 171.9, 172.0.

**Cyclo-[Lys(CIZ)-mABA]<sub>4</sub> (3d).** NH<sub>2</sub>-[Lys(CIZ)-mABA]<sub>4</sub>-OH (1.0 g, 0.056 mmol), prepared from **3c** with aqueous NaOH, was then treated with TFA/DCM, before reacting with BOP (0.246 g, 5.56 mmol) and DIEA (0.194 mL, 0.112 mmol) in DMF (55 mL). The reaction was monitored by rp-HPLC (H<sub>2</sub>O/MeCN) and, after stirring for 15 h, the solvent was removed *in vacuo*. The residue was taken up in CHCl<sub>3</sub>, washed with 1 N HCl, saturated NaHCO<sub>3</sub>, and brine, dried (Na<sub>2</sub>SO<sub>4</sub>), filtered, and solvent was removed in vacuo before chromatography on silica gel chromatography using MeOH/CHCl<sub>3</sub> (1:10) eluent to give the side chain protected octapeptide cycle **3d** (0.363 g, 39%). MS: 1662.3 (M + H)<sup>+</sup>. <sup>1</sup>H NMR (DMSO-*d*<sub>6</sub>)  $\delta$  1.44 (m, 16H), 1.80 (m, 8H), 2.99 (m, 8H), 4.54 (dd, *J* = 7.3 Hz, 7.3 Hz, 4H), 5.02 (s, 8H), 7.32 (m, 24H), 7.59 (d, *J* = 7.3 Hz, 4H), 7.79 (d, *J* = 7.4 Hz, 4H), 8.03 (s, 4H), 8.52 (d, *J* = 5.9 Hz), 10.26 (s, 4H). <sup>13</sup>C NMR (DMSO-*d*<sub>6</sub>)  $\delta$  23.4, 29.3, 31.5, 54.8, 62.9, 119.1, 122.5, 122.6, 127.6, 129.0, 129.5, 130.0, 132.6, 134.7, 135.0, 139.2, 156.2, 167.1, 171.5.

**Cyclo-[Lys(BrAc)-mABA]<sub>4</sub> (3).** The protected cyclic octapeptide **3d** (100 mg, 60  $\mu$ mol) was deprotected with HF/*p*-cresol (5 mL/0.5 mL) for 1 h at –5 °C to give the octapeptide·TFA salt (76 mg, 88%). This peptide can be purified by rp-HPLC (H<sub>2</sub>O/MeCN) and lyophilized to give unprotected cyclic octapeptide. TFA salt (13 mg, 15%). MS: 989.7 (M + H)<sup>+</sup>. HPLC: Rt = 38.6 min, 0–30% solvent B (50 min). A mixture of bromoacetic acid (45 mg, 0.32 mmol) and DCC (33.3

(15) Bruins, A. P., Covey, T. R. and Henion, J. D. *Anal. Chem.* **1987**, *59*, 2642.

(16) Iribane, J. V. and Thomson, B. A. *J. Chem. Phys.* **1976**, *64*, 2287.

mg, 0.16 mmol) in DMF (400  $\mu$ L) was stirred for 15 min and then added to a solution of the octapeptide cycle (10 mg, 10  $\mu$ mol) dissolved in DMF (200  $\mu$ L) with DIEA (14  $\mu$ L, 80  $\mu$ mol). The peptide was purified by rp-HPLC (H<sub>2</sub>O/MeCN) and lyophilized to give the bromoacetylated octapeptide cycle, template **3** (3.6 mg, 35%). MS: 1473.2 (M + H)<sup>+</sup>, 20–50% solvent B (30 min) Rt = 25.4 min.

**3,5-Di(bromoacetamido)benzoic Acid (4).** 3,5-Diaminobenzoic acid (0.300 g, 2 mmol) was dissolved in dry THF (5 mL) mixed with DMF (5 mL) and triethylamine (1.16 mL, 8.3 mmol). Bromoacetyl bromide (0.696 mL, 8.0 mmol) was added to this solution which was stirred for 2 h. The solvent was removed in vacuo, and the residue was taken up into ethyl acetate (30 mL), extracted with 3 M HCl (2  $\times$  20 mL), saturated NaHCO<sub>3</sub> (2  $\times$  20 mL), and brine (1  $\times$  15 mL), dried (MgSO<sub>4</sub>), and filtered and the solvent was removed in vacuo to give an off-white powder (**4**, 0.425 g, 55%). MS: 393.9 (M + H)<sup>+</sup>. <sup>1</sup>H NMR (DMSO-*d*<sub>6</sub>)  $\delta$  4.02 (s, 4H), 7.93 (d, *J* = 2.0 Hz, 2H), 8.16 (t, *J* = 2.0 Hz, 1H), 10.62 (s, 2H). <sup>13</sup>C NMR (DMSO-*d*<sub>6</sub>)  $\delta$  31.7, 115.1, 116.7, 133.2, 140.6, 166.5, 168.1.

**Peptide Synthesis.** Asp-Ala-Ala-Thr-Ala-Leu-Ala-Asn-Ala-Leu-Lys-Lys-Leu-[NHCH<sub>2</sub>CH<sub>2</sub>-SH] (**5**) was synthesized by manual stepwise solid-phase synthesis using HBTU/DIPEA activation and in situ neutralization for Boc-chemistry on a cysteamine linked resin.<sup>9</sup> The peptide was cleaved from the resin using liquid HF:*p*-cresol (10:1) for 1 h at 0 to –5 °C. HF was removed under vacuum, and the peptide precipitated with diethyl ether, redissolved in 20% acetic acid/H<sub>2</sub>O, diluted with H<sub>2</sub>O, and lyophilized. The peptide was purified by rp-HPLC using buffer A and a 60 min gradient from 0% to 40% B, yield 25%. rp-HPLC [Rt = 50.8 min]. MS: [obs. M + H<sup>+</sup> 1358.2; calcd 1358.8].

**General Procedure for the Synthesis of TASPs 6–9.** The ligation of the thiol peptide **5** onto templates was carried out under an inert Ar atmosphere to minimize disulfide formation. The procedure used for all TASPs is described here for TASP **6**. Template **1** (1.47 mg, 1.98 mmol) was dissolved in DMF (300 mL), and peptide **5** (in 500 mL of 100 mM Tris buffer pH 8.5) was added to the stirred solution. The mixture was stirred for 3 h and the reaction was monitored by analytical rp-HPLC and MS (Figures 1 and 2). DTT (100 mM, 100 mL) was added to the solution to reduce any disulfide present before purification by semipreparative rp-HPLC, 0–50% B over 60 min. Fractions were collected and combined according to analytical rp-HPLC, and MS then lyophilized to give TASP **6** as a white powder (7.89 mg, 68%). The compound was characterized by analytical rp-HPLC (Rt = 57.4 min) and MS ((M + H)<sup>+</sup> obs 5853.6, calcd 5852.2). TASPs **7–9** were similarly prepared and characterized from their corresponding templates **2–4**, respectively. TASP **7**: rp-HPLC: Rt = 56.2 min. MS: obs (M + H)<sup>+</sup> 5732.0, calcd 5733.2. TASP **8**: rp-HPLC: Rt = 58.0 min. MS: (M + H)<sup>+</sup> obs 6584.4, calcd 6583.6. TASP **9**: rp-HPLC: Rt = 53.9 min. MS: (M + H)<sup>+</sup> obs 2949.8, calcd 2949.6.

**Kinetics of Formation of TASP 6.** Template **1** (0.3 mg, 0.054  $\mu$ mol) and peptide **5** (3.66 mg, 2.70  $\mu$ mol) were combined in a vial fitted with a rubber septum, under Ar. Deoxygenated dioxane (1.35

mL) and 100 mM Tris buffer (1.35 mL) were added, and the mixture was stirred under an atmosphere of Ar. At regular intervals 100 mL of the solution was removed and quenched with 0.5% TFA/H<sub>2</sub>O, and stored at 4 °C until analyzed by analytical rp-HPLC 20–50% B over 50 min to separate the components. Results are summarized in Figure 2.

**Circular Dichroism.** CD data were recorded on a JASCO 710 spectropolarimeter. Peptides were dissolved in 10 mM phosphate buffer (pH 7), and measurements were made at 20.0 °C in a 3 mL cuvette with a path length of 1 cm, scanning from 250 to 190 nm every 0.10 nm.

**Sedimentation Equilibrium Studies.** Solutions (6  $\mu$ M) of each TASP (**6–8**) in 10 mM phosphate buffer (pH 7) were centrifuged at 50 000 rpm and 20 °C in a Beckman XL-A analytical ultracentrifuge. Resulting equilibrium distributions were recorded spectrophotometrically at 230 nm and analyzed using the sedimentation equilibrium equation for a single solute (MW = *M*)

$$A(r) = A(r_m) \exp[M\phi(r^2 - r_m^2)] \quad (1a)$$

$$\phi = (1 - \bar{v}\rho_s)\omega^2/(2RT) \quad (1b)$$

to obtain best fit values of *A*(*r*<sub>m</sub>), the absorbance at the air–liquid meniscus (*r*<sub>m</sub>) and the product  $\phi M$  from the dependence of absorbance upon radial distance *r*. Combination of the magnitude of the latter coefficient with the angular velocity ( $\omega$ ), universal gas constant (*R*) and absolute temperature (*T*) yielded the buoyant molecular weight, *M* (1 –  $\bar{v}\rho_s$ ), where  $\bar{v}$  is the partial specific volume of solute, and  $\rho_s$  is the solvent density.<sup>17</sup> An approximate molecular weight was obtained from a partial specific volume of 0.77 mL/g for all three solutes, this being calculated from the amino acid composition of the polypeptide component.<sup>18,19</sup> The density of the buffer, 1.000 g/mL, was also calculated from its composition.<sup>19</sup>

**Denaturation Studies.** Aliquots of 7 M GnHCl (99%, Sigma) in aqueous buffer (20 mM phosphate, pH 7.0, 0.15 M NaCl) were added to solutions of each TASP (**6–8**, 1–2 mg/mL, same buffer) in a quartz cell (0.5 mL volume, 1 cm path length). Five minutes after mixing, CD spectra were obtained at 22 °C, and the extent of denaturation was measured from the changing ellipticity at 222 nm. The fraction of unfolded TASP was plotted against [GnHCl], and the midpoint (*C*<sub>0.5</sub>) for each denaturation curve is shown in Table 1. Values for the free energy of denaturation ( $\Delta G_{\text{obs}}$ ), calculated from eq 2 using equilibrium values for denaturation (*K*<sub>D</sub>) at multiple points on each transition curve, were then plotted against the concentration (*C*) of GnHCl.<sup>20</sup> The free energy change for conversion of the TASP from its folded to unfolded form in the absence of denaturant,  $\Delta G_{\text{H}_2\text{O}}$ , was then obtained via eq 3 as the intercept after linear extrapolation to zero denaturant concentration.<sup>20</sup> Values for  $\Delta G_{\text{H}_2\text{O}}$  and the gradient (*m*) are reported for each TASP in Table 1. Due to the low concentrations of GnHCl required to denature the TASPs, errors in the linear extrapolation method<sup>20</sup> are relatively small in this case.

$$\Delta G_{\text{obs}} = -RT \ln K_D \quad (2)$$

$$\Delta G_{\text{obs}} = \Delta G_{\text{H}_2\text{O}} + m(C) \quad (3)$$

**Acknowledgment.** This work was supported by the University of Queensland and an Australian Postgraduate Research Award to A.K.W. The authors are grateful to T. Bond for amino acid analyses and Drs. West, Smythe, and Scanlon for useful discussions.

JA9719510

(17) Wills, P. R. and Winzor, D. J. In *Analytical Ultracentrifugation in Biochemistry and Polymer Science*; Harding, S. E., Rowe, A. J., Horton, J. C., Eds.; Royal Society Chemistry: Cambridge, UK, 1992; pp 311–330.

(18) Cohn, E. J.; Edsall, J. T. *Proteins, Amino Acids and Peptides as Ions and Dipolar Ions*; Reinhold: New York, 1943; pp 370–381.

(19) Laue, T. M.; Shah, B. D.; Ridgeway, T. M.; Pelletier, S. L. In *Analytical Ultracentrifugation in Biochemistry and Polymer Science*; Harding, S. E., Rowe, A. J., Horton, J. C., Eds.; Royal Society of Chemistry: Cambridge, UK, 1992; pp 90–125.

(20) (a) Ahmad, F.; Bigelow, C. C. *J. Biol. Chem.* **1982**, *257*, 12935–12938. (b) Santoro, M. M.; Bolen, D. W. *Biochemistry* **1988**, *27*, 8063–8068; 8069–8074.